Face Stability Conditions with Earth-Pressure-Balanced Shields

G. Anagnostou and K. Kovári

Abstract—Earth pressure balanced shields provide continuous support to the tunnel face using the freshly-excavated wet soil, which under pressure completely fills up the work chamber. EPB-shield tunnelling has been successfully applied worldwide in recent years. Under extremely unfavourable geological and hydrogeological conditions, however, face instabilities may occur. In this paper, the mechanism of face failure is analysed under drained conditions. Accordingly, a distinction is made between water-pressure and effective pressure in the chamber. The stability of the tunnel face is controlled through the combined effects of these two entities. The effective pressure can be visualized as a "grain to grain" contact pressure between the muck and the ground at the face. The water pressure in the chamber reduces the hydraulic head gradient in the ground and, consequently, the seepage forces acting in front of the face. The face is thus stabilized both by the direct support of the pressurized muck and by the reduction of the seepage forces in the ground. The greater the head-difference between ground and chamber, the higher the effective support pressure will have to be. A high effective support pressure has, on the other hand, operational disadvantages such as excessive cutter wear, high torque etc.. It is of great practical interest to investigate quantitatively the relationships between the effective support pressure required and the hydraulic head in the muck for a given geotechnical situation. In this contribution, normalized diagrams are provided which allow the assessment of tunnel face stability.

Résumé—Les boucliers à contrepression de terre fournissent un soutien continu du front du tunnel en utilisant la terre excavée qui, en pression, remplit complètement la chambre de travail. Ces dernières années, l'excavation de tunnels en utilisant des boucliers à contrepression de terre a été employée avec succès partout dans le monde. Cependant, des instabilités de front peuvent avoir lieu sous des conditions géologiques et géotechniques très défavorables. Dans cet article, le mécanisme d'instabilité de front a été analysé pour des conditions drainées. En conséquence, une distinction a été faite entre la pression d'eau et la pression effective dans la chambre. La stabilité du front du tunnel est assurée par les effets combinés de ces deux grandeurs. La pression effective peut être visualisée par une pression de contact "grain à grain" entre la boue et la terre en place au front. La pression d'eau dans la chambre réduit le gradient hydraulique dans le terrain et, par conséquent, les forces d'écoulement qui agissent devant le front du tunnel. Le front est donc stabilisé par le soutien direct de la boue mise en pression et par la diminution des forces d'écoulement dans le terrain. Plus la différence de pression hydraulique entre le terrain et la boue dans la chambre est grande, plus la pression effective de soutien est élevée. Cependant, une pression effective de soutien élevée a des inconvénients pratiques tels qu'usure des couteaux, grand moment de torsion, etc. Il y a un grand intérèt pratique d'analyser d'une façon quantitative les relations entre la pression effective de soutien requise et la pression hydraulique dans la boue pour une situation géotechnique donnée. Dans cet article, des abaques normalisés ont été donnés afin de pouvoir évaluer rapidement les relations entre les différents paramètres qui déterminent la stabilité du front.

1. Introduction

Tunnel construction in saturated soils is being carried out ever more frequently using closed shields, which allow the control of surface settlement and limit the risk of tunnel face failure through the continuous support of the face during excavation. Lack of sufficient face support leads, however, to tunnel-face instability. In extreme cases, the collapse propagates up to the ground surface creating a surface depression. Seepage flow towards the face may cause inadmissible surface settlement because the piezometric head in the ground decreases and the effective stresses increase. Tunnelling with closed shields such as compressed-air shields, slurry shields and earth pressure balanced shields (Stack 1982) has, therefore, a twofold aim: support of the excavation face and the reduction or prevention of seepage flow to the face.

Earth pressure shields (Fig. 1) provide continuous support of the tunnel face using freshly excavated soil, which under pressure completely fills up the work chamber (Fujita 1981; Nishitake 1990). The supporting pressure is achieved through control of the incoming and outgoing materials in the chamber, i.e., through regulation of the screw conveyor rotation and of the excavation advance rate. Considerable experience with earth-pressure shields has been gained in Japan, where this construction method was developed (Stack 1982). In 1980, earth-pressure shields were used for 27.8% of the total length of tunnel constructed in Japan, and by 1985 this figure had risen to 68% (Nishitake 1990).

In this contribution, only the problem of face stability for machine operation in EPB mode will be analysed. Neither compressed-air application (e.g., during the execution of works in the chamber), nor deformation problems (e.g., the question of settlements caused by drainage of the ground) will be discussed. Face stability conditions in slurry-shield tunnelling have been analysed in a previous paper in this journal (Anagnostou and Kovári 1994b).

Present address: Dr. G. Anagnostou and Dr. K. Kovári, Institut f. Geotechnik, Eldgenössische Technische Hochschule, CH-8093 Zürich, Hönggerberg, Switzerland.
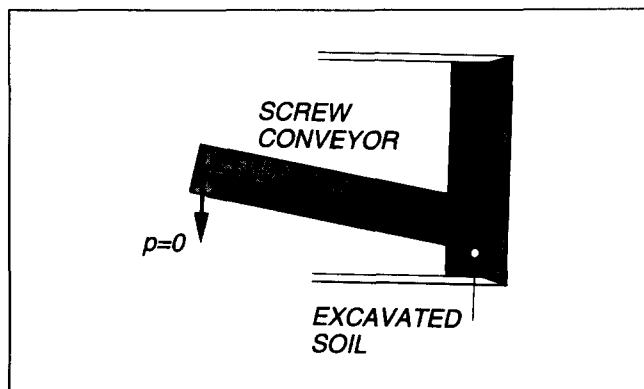
Pergamon

Figure 1. Principle of the EPB shield.

2. The Computational Model

The problem of face stability of tunnels has already been addressed by several other authors (see Krause 1987, Balthaus 1988, Leca and Panet 1988 and Leca and Dormieux 1991). In this study, a simple model which idealises the three-dimensional failure mode of the tunnel face will be used. For the sake of simplicity, the ground is considered to be homogeneous and isotropic. Deviations from these assumptions can be considered easily in more detailed numerical analyses. Face stability will be assessed by considering the limit-equilibrium of a wedge and a prismatic body, which are defined by slip surfaces beginning at the face and reaching the soil surface.

As shown in Figure 2, the circular cross-section of the tunnel is approximated by a square having the same area. This model was first proposed by Horn (1961) and is based upon the silo theory (Janssen 1895). It has also been applied to the investigation of face stability with slurry shields (Anagnostou and Kovári 1992, 1994).

Because the deformation of the ground is not being taken into account, the soil is idealised as a rigid-plastic material. The Mohr-Coulomb failure condition is assumed. The shear strength parameters, the body forces in the soil, and the boundary tractions at the tunnel-face and at the soil surface depend on whether a *drained or undrained* stability analysis is carried out (Lambe and Whitmann 1979). The question of which type of analysis is the more appropriate
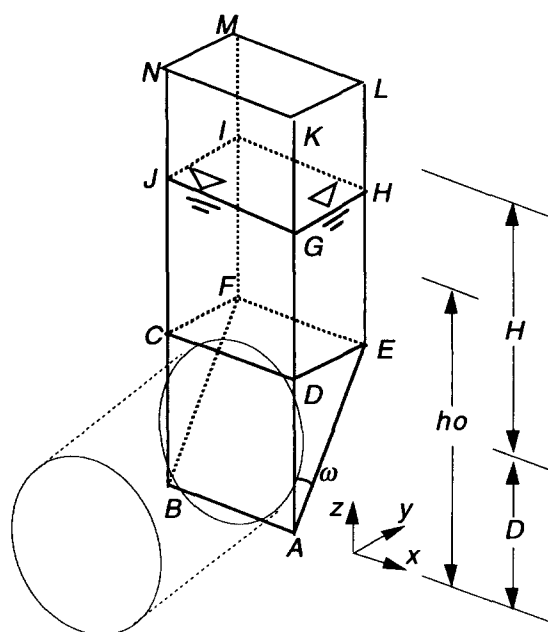
depends on the soil conditions, as well as on the excavation advance rate.

According to the results of parametric studies into the effects of the advance rate (Anagnostou 1993, 1995), drained conditions are to be expected when the permeability is higher than 10^{-7} to 10^{-6} m/sec and the net excavation advance rate is 0.1–1 m/hr or less. In a predominately sandy soil, therefore, drained stability conditions should be considered. In a clayey, low-permeability soil, undrained strength applies for assessing face stability during excavation, whereas drained conditions may be more appropriate in the case of a standstill. This paper focuses on face stability under *drained* conditions. For the case of undrained stability (Lambe and Whitmann 1979) refer to Davis *et al.* (1980).

Since a drained analysis is carried out in terms of effective stress, a distinction must be drawn between the total and effective stress acting upon the face, because the work chamber is filled with excavated soil under pressure. Only the effective normal stress can be considered as an actual support pressure. This will be termed effective support pressure and will be denoted in the following text by s'. What effects does the pore water pressure, i.e., the piezometric head h_F in the work chamber have from a stability point of view ? If it is lower than the piezometric head h_o in the undisturbed state, then the groundwater will seep through the tunnel face, and seepage forces will act towards the tunnel face (Fig. 3).

Under drained conditions, the mobilised shearing resistance t at each point on the slip surfaces is given by:

$$\tau = c/v + \sigma' \, tan\phi/v , \tag{1}$$

where c, ϕ , v and σ' denote the drained cohesion, the drained angle of internal friction, the factor of safety, and the effective normal stress, respectively. Furthermore, an additional mode of failure must be taken into consideration: Since the seepage forces are directed towards the tunnel face, tensile stresses along ABFE (Fig. 2) may also prevail. Consequently, in addition to sliding, *tensile failure* may occur when the ground lacks sufficient tensile strength. It should be noted, however, that the tensile failure mode becomes relevant only under the contradictory conditions of high cohesion and a low tensile strength (Anagnostou and Kovári 1994a,c); and, therefore, will not be considered further in this paper.

Figure 4 illustrates the forces acting upon the wedge at the face. These are:

(i)   the submerged weight G';

(ii)   the vertical force V that results from the effective normal stress σ_v' at the wedge-prism-interface CDEF;

(iii) the resultant seepage force (F_x, F_y, F_z), whereby, due to symmetry, F_y is equal to zero;

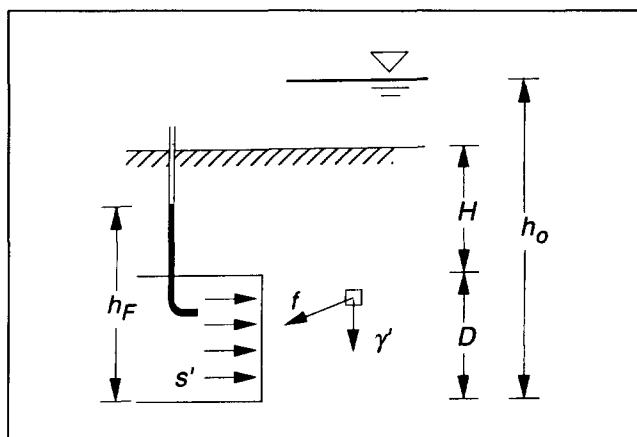*Figure 2. Sliding mechanism (after Horn 1961).*

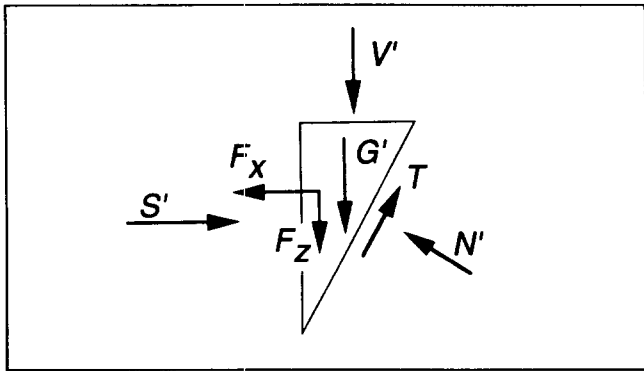*Figure 3. Seepage force f and effective support pressure s'.*

Figure 4. Forces acting upon the wedge in front of the tunnel face.

(iv) the normal force S' that results from the effective support pressure s' of the muck at the tunnel face;

(v) the normal force N' that results from the effective normal stress on the inclined sliding surface;

(vi) two horizontal normal forces resulting from the effective normal stress acting on the vertical slip surfaces ADE and BCF of the wedge;

(vii) the shear forces T on the inclined as well as on the vertical sliding surface activated by relative movement. No shear force will be considered as acting on the internal slip surface DEFC.

The vertical force V' is computed by applying Janssen's silo-formulae to the prismatic body, taking into account the seepage forces acting within the prismatic body (see Appendix). The frictional part of the shear strength on the vertical sliding surfaces depends essentially on the corresponding effective horizontal stresses (σ_x', σ_y'). Following Janssen's silo-theory, a constant ratio λ of horizontal to vertical stresses along the slip surfaces of the prism, as well as that of the wedge, will be assumed. The value of λ is taken to be 0.80 for the prism and 0.40 for the wedge (Anagnostou and Kovári 1994b). The linear approximation proposed in the German Standards for slurry walls (DIN 4126) will be adopted for the vertical stress distribution $\sigma_z'(z)$ along the slip surfaces ADE and BCF of the wedge,

Determination of the seepage forces {Fx, Fz} calls for a *numerical seepage-flow analysis*. Such a calculation yields the three-dimensional steady-state potential field. Darcy's law will be assumed for modelling seepage-flow. The permeability constant does not, however, influence the steady state head field. The computation is based upon the following boundary conditions. At the tunnel face, a constant piezometric head $h_F \le h_o$ is prescribed. In the extreme case, the tunnel face represents a seepage face, i.e., the pressure is atmospheric and the piezometric head equal to the elevation at each point ($h_F = z$). At a sufficient distance from the tunnel face (the far-field boundary condition), the piezometric head corresponds to the water table elevation (h_o). Assuming a waterproof tunnel lining, a no-flow boundary condition applies to the tunnel walls. For all of the numerical examples in this paper, it will be assumed that, in spite of drainage through the face, there is no drawdown of the water table. This involves a continuous groundwater recharge by, e.g., rainfall or an adjacent river, lake or well.

The numerical calculations were carried out by the three-dimensional finite element code HYDMEC (Anagnostou 1991). Figure 5 shows the central part of the finite element mesh that will be used in the numerical examples in this paper, taking the symmetry of the system into account. Consider a tunnel having a diameter of 10 m and an overburden of 20 m. The groundwater table is at the level of the ground surface. The tunnel face is under atmospheric pressure.

Figure 6a represents the contour lines of the piezometric head in the vertical plane of symmetry. In this example, the pressure in the chamber is atmospheric. The increasing density of the potential lines close to the tunnel face indicates an increasing value of the seepage forces. This is also demonstrated when plotting the pore water pressure along the tunnel axis (Fig. 6b). As the seepage forces are oriented perpendicularly to the potential lines, the resultant seepage force acting on the wedge slopes slightly downward, while that in the prism above is practically vertical. The destabilizing effect of the seepage forces acting on the wedge is thus clearly apparent. An approximately horizontal load is exercised on the wedge, while the vertical load from the prism is simultaneously increased.

The face stability analysis proceeds in three steps:

(i) Determination of the three-dimensional hydraulic head-field $h(x,y,z)$ for given geometric (diameter, overburden) and boundary conditions (the piezometric head in the chamber, elevation of the water table) by means of a finite element computation.

(ii) Computation of the forces acting upon the wedge for a specific collapse mechanism (i.e., for a given inclination ω of the slip surface ABFE). This step includes numerical integration of the seepage forces within the wedge and the prism based upon the piezometric head-field calculated in step (i) (see Appendix).

(iii) Computation of the necessary effective face support force by applying the conditions of equilibrium and the failure criteria on the slip surfaces.

The critical inclination ω_{cr} of the sliding surface is determined by iteratively maximizing the support force, i.e., by repeating steps (ii) and (iii) with different angles of inclination w. Step (i) has to be carried out only once, whereas steps (ii) and (iii) are carried out simultaneously because the resultant seepage forces must be recomputed for each value of ω.

3. The Necessary Effective Support Pressure

At limit equilibrium, the effective support pressure s' depends on the tunnel diameter D, on the overburden H, on the piezometric head in the chamber h_F, on the elevation of the water table h_o, on the effective shear strength parameters c and ϕ, on the submerged unit weight γ' (for soil
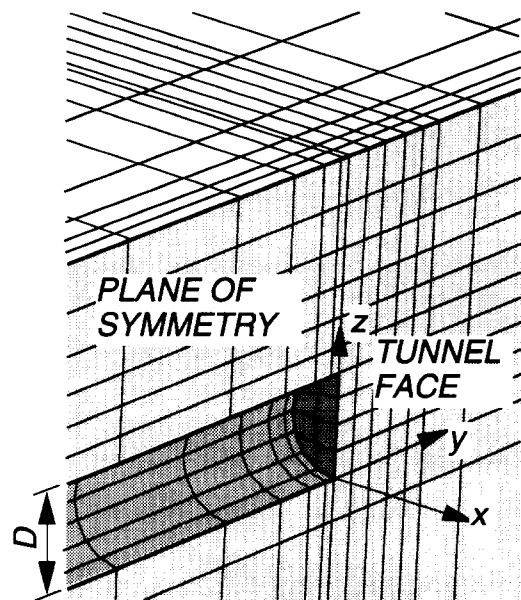

Figure 5. Finite-element mesh for the computation of the head field.

beneath the water table) and on the dry unit weight γ_d (for the soil above the water table), i.e.,

$$s' = f(D, H, h_F, h_o, c, \phi, \gamma', \gamma_d) . \qquad (2)$$

According to the equilibrium equations, the effective support pressure depends linearly on the size of the forces acting upon the wedge. According to the Mohr-Coulomb yield criterion, the shear forces depend linearly on the cohesion. Furthermore, the seepage forces are proportional to the head gradients and, due to the linearity of Darcy's law, to the head difference $(h_o - h_F)$ as well. For these reasons, a linear relationship holds between effective support pressure s', cohesion c and head difference $\Delta h = h_o - h_F$. By carrying out a dimensional analysis, one obtains the following general form of the limit equilibrium condition:

$$s' = F_o \gamma' D - F_1 c + F_2 \gamma' \Delta h - F_3 c \frac{\Delta h}{D} , \qquad (3)$$

where F_o to F_3 are dimensionless coefficients that depend on the friction angle ϕ, on the geometric parameters H/D and $(h_o-D)/D$, and on the ratio of the dry to the submerged unit weight γ_d / γ'. In spite of the linear relationship between s' and Δh, the undisturbed piezometric head h_o is an independent parameter because it affects the size of the flow domain. The term $F_o \gamma' D$ in eq. (3) is equal to the necessary support pressure in a cohesionless ground $(c = 0)$ when seepage forces do not occur $(\Delta h = 0)$, i.e., when the groundwater pressure is completely compensated by the fluid pressure in the chamber (see, e.g., Passante Ferroviario

Figure 6. Result of seepage calculations in the vicinity of the tunnel face. (a) Contour-lines of piezometric head. (b) Porewater pressure distribution along the tunnel axis.

Milano, Peron and Marcheselli 1995). In this case, the support pressure increases linearly with the tunnel diameter. The other three terms express, for a given value of ϕ, the general linear dependency of support pressure s' on cohesion c and head difference Δh.

Figure 7 shows the coefficients F_o to F_3 as functions of the friction angle ϕ. The diagrams have been computed numerically with the model described in Section 2. The curves cover the relevant range of the geometric parameters H/D and $(h_o-D)/D$. The ratio γ_d / γ' was taken to 1.60, a good enough approximation for practical purposes. The solid lines in the diagram for F_o apply to cases where the water level is at the surface or above it $(h_o \geq H+D)$, e.g., under a seabed or river. The dashed lines hold when the groundwater table is in a distance of $D/2$ above the tunnel crown.

Figure 7 shows that the overburden does not have any effect on the normalized support pressure F_o when $H/D > 2$ or $\phi > 25°$. The coefficient F_1 (i.e., the effect of cohesion in the absence of seepage forces) does not depend on the elevation of the water table. The influence of the overburden on F_1 is small. The coefficient F_2 expresses the effect of head difference on support pressure in a cohesionless soil, and depends solely on the size of the flow domain above the crown, i.e., on $(h_o-D)/D$ or, when the water level is above the soil surface on H/D. The coefficient F_3 (the cross effect of cohesion and head difference) depends both on the overburden H/D and on the elevation of the water table (ho-D)/D. Because the influence of H/D on F_3 amounts to less than 5%, it not been included in the diagram.

The formula (3), together with the diagrams in Figure 7, provide a simple but powerful tool to characterize quantitatively the face stability at EPB operation in a given particular case.

Comparison with Experimental Results

Chambon and Corté (1994) have conducted centrifugal model tests concerning face stability in dry cohesionless soils. Predictions based on the model proposed in this paper are compared with the measured values from the tests. Figure 8 shows the empirically determined support pressure at collapse as a function of tunnel diameter (dashed line). The values of support pressure are very low due to the high friction angle of the model material (ca. 40°). In the model tests, the overburden was equal to 4D, the dry unit weight was equal to 16.1 kN/m³, and the soil had a cohesion and a friction angle in the range 0–5 kPa and 38–42°, respectively. The theoretical minimum face support pressure for tunnelling in dry soil is given by the following equation:

$$s = F_o \gamma_d D - F_1 c . \qquad (4)$$

This equation is similar to (3), the only difference being that the dry unit weight γ_d is used instead of the submerged unit weight γ'. The two solid lines with the black markers in Figure 8 show the support pressure according to (4) for $c = 0$ and $c = 5$ kPa, respectively. The lines have been computed for an average friction angle of $\phi = 40°$. The solid lines with white markers have been obtained using the model of Leca and Dormieux (1990). Both models yield satisfactory estimates of the experimental values. The results discussed above concerning the effects of the overburden and of tunnel diameter are also in accordance with the experimental findings.

4. Case Study—The Storebælt Railway Tunnel

The Great Belt project (Biggart et al. 1993) involves two single-lane tunnels bored by four EPB-shielded tunnel boring machines. The tunnels cross glacial tills and fissured marls (Fig. 9). The upper till is a preconsolidated undisturbed soil with up to 20% clay. The lower till is an extremely heterogeneous material containing irregular sand lenses, gravels and glacial boulders. Due to the high
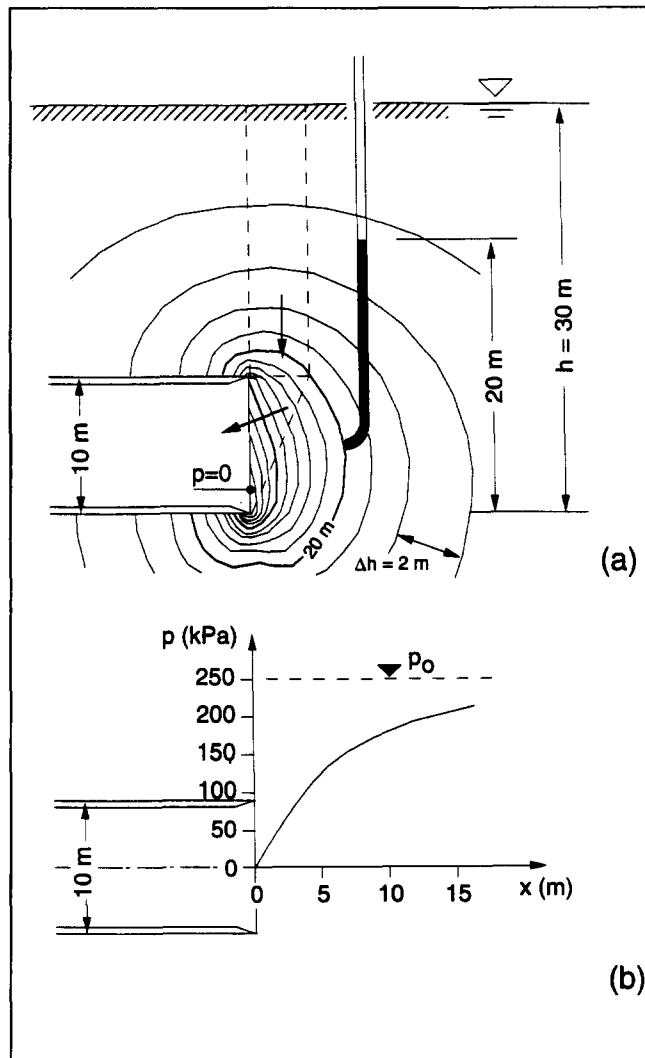
H/D=
1.0
≥5
2
0.8
≥5
2
0.6
1
1
F_o
0.4

[inset diagram: H, D, h_o water table]

0.2
$h_o ≥ H+D$
$h_o = 1.5 D$
0

15   20   25   30   35
Friction Angle   φ [°]

0.8
$\left\{ \begin{array}{l} = H/D, \text{ if } h_o > H+D \\ = (h_o-D)/D \text{ if } h_o < H+D \end{array} \right.$
0.7
0.5
1
F_2 0.6
≥3
0.5
0.4

15   20   25   30   35
Friction Angle   φ [°]

5
H/D=
≥5
4
2
1
F_1
3
2

15   20   25   30   35
Friction Angle   φ [°]

0.12
0.10
0.08
≥3
F_3 0.06
1
0.04
0.5
$\left\{ \begin{array}{l} = H/D, \text{ if } h_o > H+D \\ = (h_o-D)/D \text{ if } h_o < H+D \end{array} \right.$
0.02
0.00

15   20   25   30   35
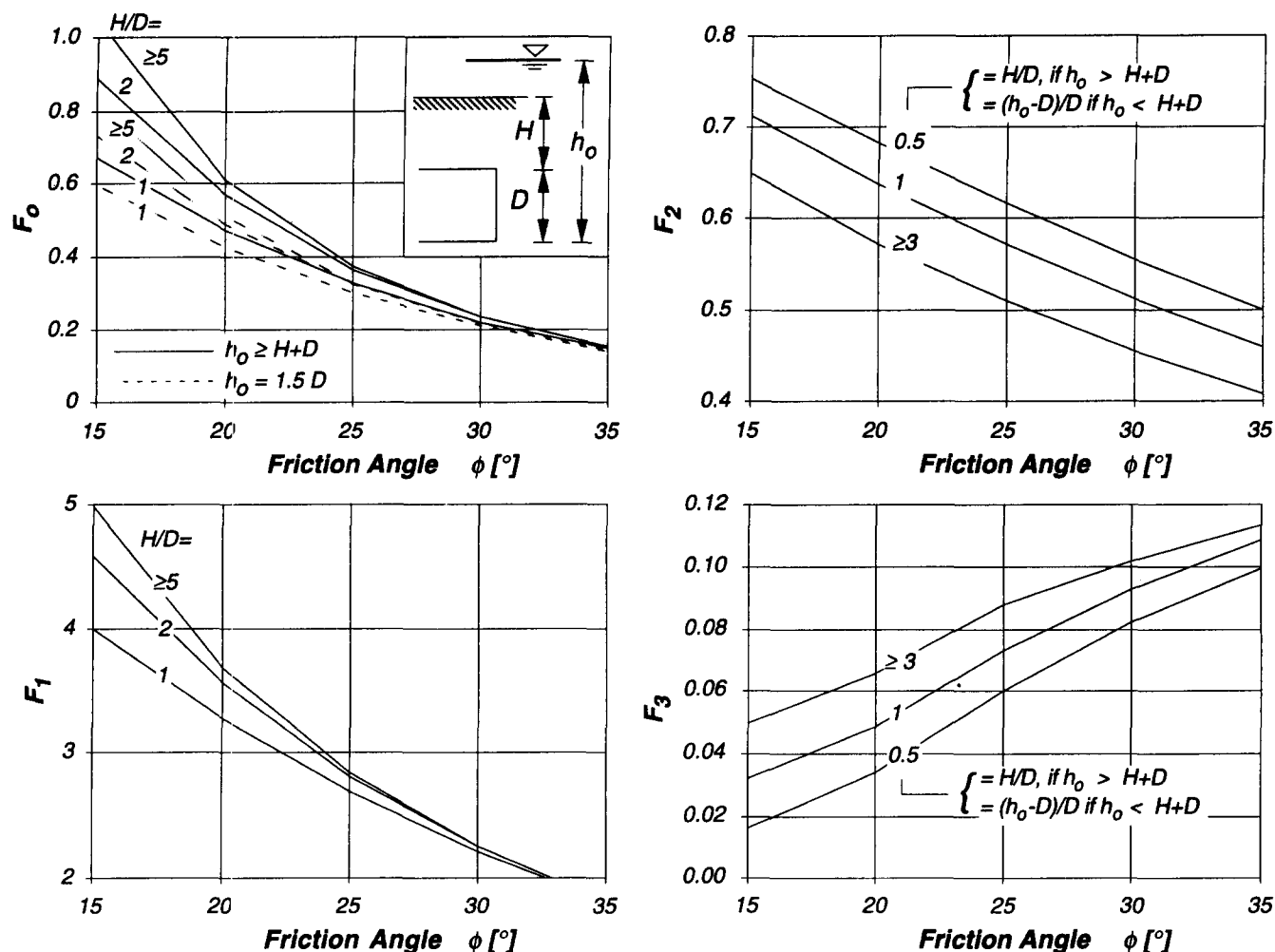**Friction Angle   φ [°]**

Figure 7. Nomograms for the dimensionless coefficients F_o to F_3.

porewater pressures (up to 4 bar in the tills), extensive drainage works have been carried out. This so-called "Moses" project reduced the seepage forces, simplified cross-passage constructions, and made entry into the working chamber possible at low air pressure. Detailed information on the Storebælt project has already been given (Biggart et al. 1993, Darling 1993, Sternath 1994).

In order to provide a better understanding of face stability conditions, stability calculations have been performed based on the model described above (Kovári and Anagnostou 1994). Both drained and undrained conditions have been studied. Drained conditions are relevant because of the high permeability of the till, as indicated by the rapid response of the piezometric heads observed after the installation of the pumps in the Moses project. In the following, the interaction between the main factors will be demonstrated by means of a parametric study concerning station 12'800 (Fig. 9). The depth of cover and the sea depth amount here to approximately 30 m and 10 m, respectively. In the model, the circular tunnel section (diameter 8.70 m) has been approximated by a rectangular one with a side-length of D=7 m. The limit equilibrium condition between effective support pressure s', cohesion c and head difference $(h_o - h_F)$ can be obtained from eq. (3) and the diagrams of Figure 7, with φ = 32.5° and γ' = 13 kN/m³:

$$s' = 18 - 2\,c + 5.6\,(h_o\text{-}h_F) - 0.016\,c\,(h_o\text{-}h_F)\ ; \qquad (5)$$

units in [kPa] and [m]

Figure 10 shows the graph of eq. (5). Note that the compensation of the water pressure (i.e., $h_o = h_F$) suffices

for face stability even when the ground shows a cohesion c as low as 10 kPa. Furthermore, it may be seen that in a cohesionless ground, the same reduction in the required effective support pressure of approx. 56 kPa can be achieved either by reducing the head difference by 10 m (1 bar) or by increasing the ground cohesion by approximately 28 kPa. In other words, the effects of $\Delta s' \cong$ 56 kPa, $\Delta(h_o - h_F) =$ 10 m and $\Delta c \cong$ 28 kPa in stabilizing the tunnel face are statically equivalent. According to Figure 10, when reducing the head difference by 20 m in a ground with a cohesion of c = 30 kPa, the required effective face support s' decreases from approximately 160 kPa to 60 kPa. Therefore, the lowering of the piezometric head into the ground by pump operation represents an extremely effective measure for face stabilisation in cases with exceptionally high piezometric heads.

In view of the great importance of the piezometric head h_F in the chamber, the principle of the so-called "water-pressure-type EPB shield" is immediately obvious. For this type of machine, the piezometric head should be maintained through the application of pressurized water in the work chamber (Abe et al. 1978; Fujita 1981; Stack 1982). Moreover, face stability conditions could be satisfied by maintaining a water pressure in the chamber greater than the pore water pressure in the ground. The necessary "negative" head difference Δh can be computed from eq. (5) by setting s'=0. In the present study (and assuming a cohesionless ground), the head in the chamber should be 3–4 m higher than the sea level in order that the effective support pressure s' is equal to zero. Whether this solution is practicable or not depends on the permeability of the ground
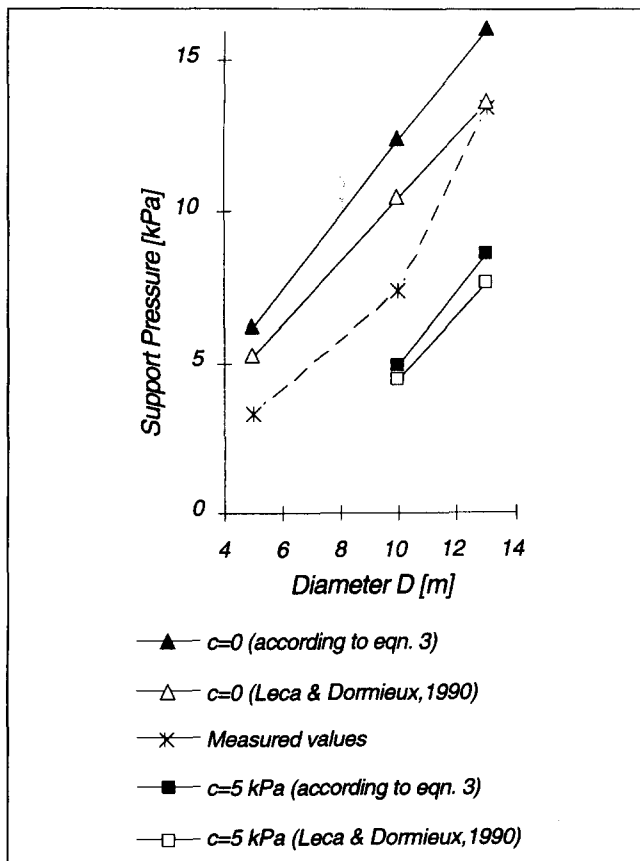
Figure 8. *Experimentally determined and computed support pressures as a function of tunnel diameter for dry conditions.*

and of the muck: the more permeable the ground and the muck, the higher the pressurized water losses towards the ground and the screw conveyor will be; and the more water will have to be transported, together with the solid matter, out of the tunnel.

5. The Operational Implications of a High Effective Support Pressure s'

If the difference between the water level h_o and the head h_F in the chamber for some reason cannot be kept low, the effective support pressure s' to ensure face stability will be high. However, at high effective support pressure, the muck in the chamber does not behave as a viscous fluid leading to a fluctuation of the distribution of the effective pressure acted on the face (Fig. 11a). If locally the pressure s' becomes very low, a cave-in involving progressive instability of the face may occur.

Another implication of high effective support pressures arises from the large shear resistance of the compressed muck against the rotating cutting wheel. The latter not only excavates the ground at the face, but also, with each rotation, shears the compacted muck in the chamber, resulting in significant wear of the whole cutter head and excessive torque (Fig. 11b).

The third disadvantage of a high effective support pressure stems from the possible arching of the muck at the entrance to the screw conveyor (Fig. 11c), thereby inhibiting the discharge (Fujita 1981). If it is not noticed by the operator in time, the muck becomes much more compacted. None of these operational difficulties occurs when the muck in the chamber acts as a viscous fluid.

Two possible ways of reducing the seepage forces may be considered: (1) By decreasing the pore water pressure in the ground; and (2) by maintaining a sufficient head h_F in the chamber. The latter method depends upon the combined effects of ground properties, muck properties and machine-specific details.

Consider the system represented by the machine and the surrounding ground (Fig. 12), and let k_o and k denote the permeability of the ground and of the muck, respectively. The piezometric head at a large distance from the tunnel face corresponds to the undisturbed groundwater table h_o, and at the exit of the screw conveyor is equal to h_A. The piezometric head difference $h_o - h_A$ is dissipated partially within the ground and partially within the machine. If the muck is much more permeable than the undisturbed soil ($k \gg k_o$), then the head difference will be dissipated mainly within the ground ahead of the face. In the extreme case, the hydraulic potential within the machine is equal to the head h_A at the exit of the screw conveyor. The lower the permeability of the muck, the larger the portion of the head difference dissipated within the machine, and the higher will be the piezometric head in the work chamber. In the borderline case of a very low-permeability muck ($k \ll k_o$), the hydraulic head h_F at the tunnel face corresponds to the undisturbed piezometric head h_o and decreases along the screw conveyor to the value h_A.

Apart from the injection of pressurized water into the chamber (see end of Section 4), two basic possibilities for maintaining a high water pressure in the work chamber arise from these considerations: either (1) by maintaining a high piezometric head at the exit of the screw conveyor, or (2) by decreasing the permeability of the muck. The first solution requires either the maintenance of a soil plug or the installation of a pump at the discharge port of the screw conveyor. For the formation of a plug, various "water-cut-off" devices have been developed (Nishitake 1990). However, plug formation presupposes a predominately clayey, compressible muck. In a sandy or gravelly soil, a high pressure can be maintained only through a pump, but the excavation advance rate may then become dependent on the performance of the pump.
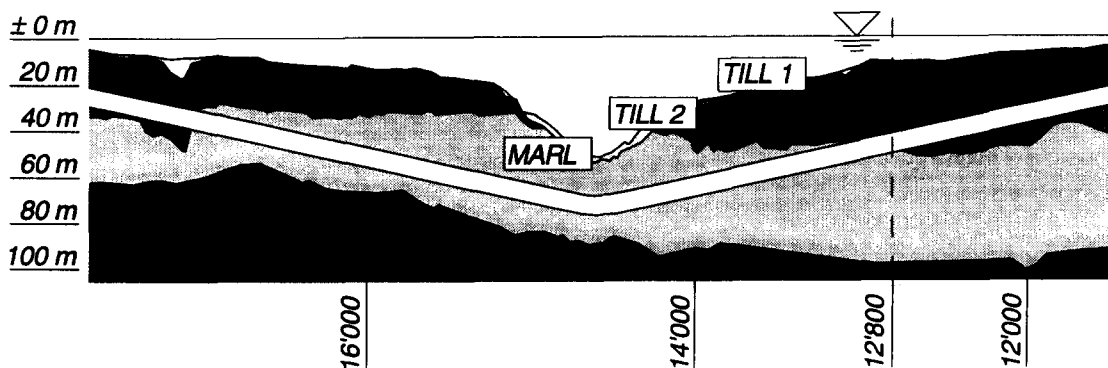

Figure 9. *Geological profile of the Storebælt railway tunnel (after Biggart et al. 1993).*
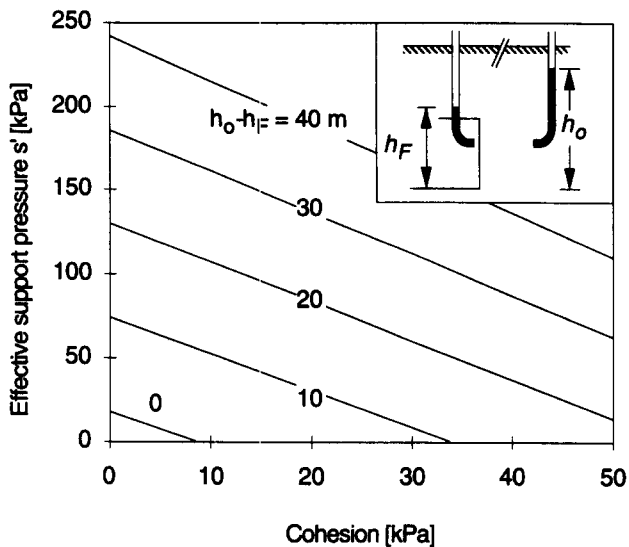
Figure 10. Effective support pressure as a function of cohesion c and of hydraulic head difference (h_o-h_F) for a given chainage of the Storebælt Tunnel.
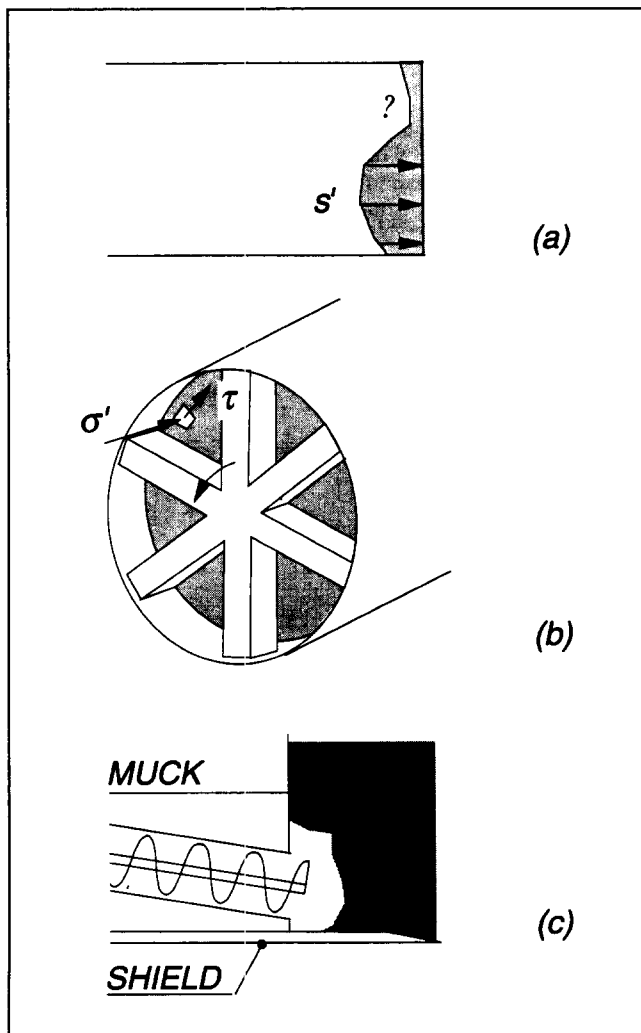

Figure 11. Problems caused by a high effective support pressure s' and a high friction angle of the muck. (a) Uncontrollable support pressure distribution; (b) Excessive cutter-wear and torque; (c) Arching at the entrance to the screw conveyor.

The addition of bentonite suspensions or polymers to the excavated material (conditioning) can reduce both its permeability and shear strength (internal friction angle) (Babendererde 1989, Nishitake 1990, Babendererde and Babendererde 1995). Similar muck treatment problems may then be encountered as for slurry shields. Environmentally acceptable additives recently have been developed for use in conditioning. The importance of thoroughly mixing the excavated material in the work chamber is especially great with an inhomogeneous ground (Anagnostou and Kovári 1994a). For high piezometric heads, the only reliable solution is the installation of a pump.

6. Closing Remarks

When using an EPB-shield, a distinction must be drawn between the effective stress s' acting on the tunnel face and the pore water pressure p in the work chamber. The stability of the tunnel face is guaranteed through the joint effects of s' and p. The larger the pore pressure p, the smaller the necessary effective support pressure s', and vice-versa. Consequently, when using an earth pressure shield, both the effective support pressure s' and the pore water pressure p should be controlled and adjusted according to the hydrological and soil mechanics conditions encountered. Contrary to the situation with compressed air and slurry shields, where only one parameter has to be regulated (air or slurry pressure, respectively), two such parameters exist for earth pressure shields. However, they may be difficult to control in practice. Because both parameters depend on the characteristics of the excavated ground, the way the ground is mixed in the work chamber, the rotational speed of the screw conveyor, and the excavation advance rate, both geotechnical and operational aspects will affect tunnel face stability.
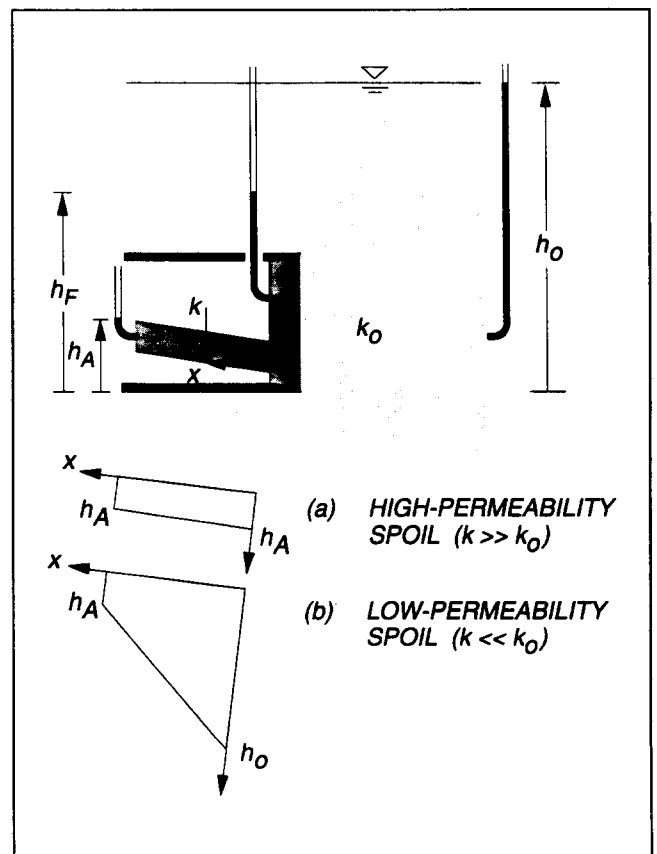

Figure 12. Loss of head difference within the ground and along the screw conveyor: (a) High-permeability muck; (b) Low-permeability muck

For operational reasons, the shear resistance of the muck should be kept as low as possible. Depending on the soil encountered during tunnel excavation, conditioning by means of lubricants (rheological foams, polymers, etc.) may be necessary in order to reduce its friction angle. The shear resistance of the muck also can be reduced by maintaining a low effective stress s' in the chamber. In this case, the head difference between the chamber and the ground should be kept as small as possible in order to ensure face stability. This can be achieved either by reducing the permeability of the muck within the working chamber (with additives and thorough mixing), or through additional measures (such as the installation of a pump at the exit of the screw conveyor).

Acknowledgments

References

Abe, T.; Sugimoto, Y.; and Ishihara, K. 1978. Development and application of environmentally acceptable new soft ground tunnelling method. *Proc. Int. Symp. "Tunnelling Under Difficult Conditions", Tokyo*, 315–320.

Anagnostou, G. 1991. Untersuchungen zur Statik des Tunnelbaus in quellfähigem Gebirge. Dissertation Nr. 9553, Eidg. Techn. Hochschule Zürich (in German).

Anagnostou, G. and Kovári, K. 1992. Ein Beitrag zur Statik der Ortsbrust beim Hydroschildvortrieb. In *Tunnelbau-Symposium "Probleme bei maschinellen Tunnelvortrieben? Gerätehersteller und Anwender berichten"*, TU München (in German).

Anagnostou, G. 1993. Modelling seepage flow during tunnel excavation. *Proc. ISRM International Symposium - EUROCK '93, "Safety and Environmental Issues in Rock Engineering", 21–24/06/1993, Lisbon, Vol. 1*, 3–10. Rotterdam: A. A. Balkema.

Anagnostou, G. and Kovári, K. 1994a. Die Stabilität der Ortsbrust bei Erddruckschilden. In *Stabilitätsprobleme in der Geotechnik, Frühjahrstagung der Schweiz Gesellschaft für Boden- und Felsmechanik* **29**, April 1994, Mitt. der SBGF 129, 27–34 (in German).

Anagnostou, G., Kovári, K. 1994b. The Face Stability of Slurry-shield-driven Tunnels. *Tunnelling and Underground Space Technology* 9(2), 165–174.

Anagnostou, G., Kovári, K. 1994c. Stability analysis for tunnelling with slurry and EPB shield. *Proc. Gallerie in condizioni difficili, Torino, 29.11–1.12.94*.

Anagnostou, G. 1995. Influence of tunnel excavation on hydraulic head. *Int. Journal of Num. and Analyt. Meth. in Geomechanics*, 19, 725–746.

Babendererde, S. 1989. Stand der Technik und Entwicklungstendenzen beim maschinellen Tunnelvortrieb im Lockerboden. STUVA, *Forschung+Praxis* 33, 78–84 (in German).

Babendererde, S. and Babendererde, L. 1995. Advanced Techniques for EPB-TBM Operation. *Tunnels et Ouvrages Souterrains* **128**, 79–82.

Balthaus, H. 1988. Standsicherheit der flüssigkeitsgestützter Ortsbrust bei schildvorgetriebenen Tunneln. In: *Festschrift H. Duddeck. Inst. für Statik TU Braunschweig*, 477–492 (in German).

Biggart, A. P.; Rivier, J.-P.; and Sternath, R. 1993. Storebælt Railway Tunnel—Construction. *Proc. Int. Symp. on Technology of Bored Tunnels under Deep Waterways, Copenhagen, Denmark*, 63–93.

Chambon, P. and Corté, J.-F. 1994. Shallow Tunnels in Cohesionless Soil: Stability of Tunnel Face. *Journal of Geotechnical Engineering* 120(7), 1148–1165.

Darling, P. 1993. Coming clean over Storebaelt. *Tunnels & Tunnelling* 10, 18–26.

Davis, E. H.; Gunn, M. J.; Mair, R. J.; and Seneviratne, H. N. 1980. The stability of shallow tunnels and underground openings in cohesive material. *Geotechnique* 30(4), 397–416.

DIN-4126. 1986. Ortbeton-Schlitzwände. Konstruktion und Ausführung (in German).

Distelmeier, H. 1987. Tunnelauskleidungen hinter grundwasserverdrängenden Schildvortriebmaschinen. *Bauingenieur* **62**, 487–492 (in German).

Eisenstein, Z.D. 1993. Large undersea tunnels and the progress of tunnelling technology. *Proc. Int. Symp. on Technology of Bored Tunnels Under Deep Waterways, 3–5 Nov. 1993, Copenhagen, Denmark*.

Fujita, K. 1981. Use of Slurry and Earth-Pressure-Balance Shield in Japan. *Int. Congress on Tunnelling, Tunnel 81, Bd. 1*, 383–406. Düsseldorf. (Ed.: Düsseldorfer Messegesellschaft mbH - NOWEA - in Zusammenarbeit mit der Deutschen Gesellschaft für Erd- und Grundbau e.V.)

Horn, M. 1961. Alagutak homlokbiztositására ható vizszintes földnyomásvizsgálat néhány eredménye. Az országos mélyépitőipari konferencia elóadásai, Közlekedési Dokumentációs Vállalat, Budapest (in Hungarian). See also "Horizontaler Erddruck auf senkrechte Abschlussflächen von Tunneln", in Landeskonferenz der ungarischen Tiefbauindustrie, Budapest (German translation, STUVA, Düsseldorf).

Janssen, H. A. 1895. Versuche über Getreidedruck in Silozellen. *Zeitschrift des Vereins deutscher Ingenieure* **XXXIX** (35), 1045–1049 (in German).

Kovári, K. and Anagnostou, G. 1994. "Storebælt Railway Tunnel - Assessment of face stability." Report prepared for the MT-Group, Consortium for Storebælt Crossing.

Krause, T. 1987. Schildvortrieb mit flüssigkeits- und erdgestützter Ortsbrust. Dissertation TU Braunschweig. (in German)

Lambe, T. W. and Whitman, R. V. 1979. *Soil Mechanics, SI Version*. New York: John Wiley & Sons.

Leca, E. and Dormieux, L. 1990. Upper and lower bound solutions for the face stability of shallow circular tunnels in frictional material. *Géotechnique* **40**, 581–606.

Leca, E. and Panet, M. 1988. Application du calcul à la rupture à la stabilité du front de taille d' un tunnel. *Revue Française de Géotechnique* **43**, 5–19 (in French).

Nishitake, S. 1990. Advanced technology realize high-performance earth pressure balanced shield. In *Franchissements souterrains pour l'Europe*, 291–302, (M. Legrand, ed.). Rotterdam: A.A. Balkema.

Peron, J. Y. and P. Marcheselli. 1995. La construction du tunnel ferroviaire de la liaison Passante Ferroviario a Milan. *Tunnels et Ouvrages Souterrains* **128**, 130–138.

Stack, B. 1982. *Handbook of Mining and Tunnelling Machinery*. Chichester, U.K.: John Wiley & Sons.

Sternath, R. 1994. Geotechnische Sonderverfahren für die Vortriebe des Eisenbahntunnels unter dem Grossen Belt. *Baugrundtagung*, 175–195. Köln (in German).

Notations

c	=	drained cohesion
D	=	diameter of tunnel
$f_{x,y,z}$	=	Seepage forces per unit volume
$F_{x,y,z}$	=	Seepage forces
$F_{0,1,2,3}$	=	Coefficients in the drained stability condition
H	=	overburden
h	=	piezometric head
h_F	=	piezometric head in the chamber
h_o	=	elevation of water table
s	=	support pressure
s'	=	effective support pressure
γ'	=	submerged unit weight
γ_d	=	dry unit weight
Δh	=	$h_o - h_F$
λ	=	coefficient of lateral pressure
ν	=	safety factor
σ_z'	=	vertical effective stress
ϕ	=	drained angle of internal friction
ω	=	inclination of slip surface
ω_{cr}	=	inclination of critical wedge

APPENDIX A. The Seepage Forces

The seepage forces per unit volume (f_x, f_y, f_z) are equal to the gradient of the numerically computed hydraulic head $h(x,y,z)$:

$$f_x = -\gamma_w \,\partial h/\partial x, \quad f_y = -\gamma_w \,\partial h/\partial y, \quad f_z = -\gamma w \,\partial h/\partial z \ . \qquad (6)$$

The resultant seepage force (F_x, F_y, F_z) acting on the wedge is obtained by applying Gauss's theorem to the body force integrals over the wedge volume:

$$F_x (\omega) = \gamma_w \left(-\cos\omega \int_{ABFE} h^* \, ds + \int_{ABCD} h^* \, ds \right), \qquad (7)$$

$$F_z (\omega) = \gamma_w \left(\sin\omega \int_{ABFE} h^* \, ds - \int_{CDEF} h^* \, ds \right), \qquad (8)$$

where ω is the shear plane inclination (Fig. 2); the integral-symbols denote integration over the indicated surfaces ABFE, ABCD, CDEF (Fig. 2); and h^* is the average head over the direction y within the wedge:

$$h^* = h^* (x,z) = \frac{1}{D} \int_{-D/2}^{D/2} h(x,y,z) \, dy \ . \qquad (9)$$

Due to symmetry, the y-component of the resultant seepage force is equal to zero.

The average effective vertical stress σ_v' at the wedge-prism-interface CDEF is computed according to silo-theory (Janssen 1895), the seepage forces being introduced into the equilibrium equation.

Water Level above Soil Surface

For the sake of simplicity, the case of a water level above the soil surface $(h_o \geq H + D)$ will be considered first. In terms of effective stresses, the vertical equilibrium equation reads as follows:

$$\frac{d\sigma_z'}{d_z} - \frac{\lambda \tan\phi}{R} \sigma_z' = \frac{c}{R} - \gamma' - f_z^{**}, \qquad (10)$$

where R denotes the ratio of the area to the circumference of a horizontal cross-section of the prism; and f_z^{**} is the vertical seepage force averaged over the horizontal prism-section at the elevation z:

$$R = \frac{D \tan\omega}{2(1 + \tan\omega)}, \qquad (11)$$

$$f_z^{**} = \frac{1}{D^2 \tan\omega} \int_0^{D\tan\omega} \int_{-D/2}^{D/2} f_z(x,y,z) \, dy \, dx \ . \qquad (12)$$

Solving eq. (10) yields the following formula for the vertical effective stress sv' acting on the wedge $(z=D)$:

$$\sigma_v' = \frac{R\gamma' - c}{\lambda \tan\phi} (1 - e^{-\lambda \tan\phi \, H/R}) + \gamma_w \, \alpha \ , \qquad (13)$$

where

$$\gamma_w \, \alpha = \int_D^{D+H} f_z^{**} e^{-\lambda \tan\phi(z-D)/R} \, dz \ . \qquad (14)$$

The first term in eq. (13) gives the effective vertical stress

according to the classical silo-theory (without seepage); the second term $(\gamma_w \alpha)$ denotes its increase due to the seepage. Eq. (14) reveals that:

- In the supposed case of a ground without internal friction $(\lambda \tan\phi = 0)$, the seepage-induced increase in σ_v' is obtained by integrating the average seepage force over the height of the prism. For example, in the case with a constant seepage force f, the increase in σ_v' amounts to $f \cdot H$.

- In the general case with $\lambda \tan\phi = 0$, the increase in σ_v' due to seepage is obtained by integrating a weighted seepage force over the height of the prism. The weighting factor $e^{-\lambda \tan\phi \, (z-D)/R}$ is equal to 1 at $z = D$ (i.e., at the wedge-prism interface CDEF) and decreases exponentially with increasing distance $(z-D)$ from the tunnel. The higher the frictional resistance $(\lambda \tan\phi)$, the more rapidly this factor decreases. Accordingly, the seepage-induced part of the effective stress σ_v' is dominated by the seepage forces in the vicinity of the tunnel crown.

By means of Gauss's theorem, one obtains the following equation from (14):

$$\alpha = h_o \, e^{-\lambda \tan\phi H/R} - h^{**} (D) + \frac{\lambda \tan\phi}{R} \int_D^{D+H} h^{**} (z) \, e^{-\lambda \tan\phi(z-D)/R} \, dz \ , \qquad (15)$$

where $h^{**}(z)$ denotes the average hydraulic head at the horizontal prism-section at the elevation z:

$$h^{**} (z) + \frac{1}{D^2 \tan\omega} \int_0^{D\tan\omega} \int_{-D/2}^{D/2} ? \, h (x,y,z) \, dy \, dx \ . \qquad (16)$$

This equation is more convenient than (16) for the numerical computation because it does not contain gradients of head.

Water Level below Soil Surface

When the water level is below the soil surface $(h_o < H+D)$, the prism must be divided into two parts. Applying silo-theory to the upper part yields the vertical stress acting at the level of the water table $(z=h_o)$:

$$\sigma_z' (h_o) = \frac{R\gamma_d - c}{\lambda \tan\phi} (1 - e^{-\lambda \tan\phi (H + D - h_o)/R} \ , \qquad (17)$$

where γ_d denotes the dry unit weight. The stress σ_v' at the prism-wedge interface is obtained by solving the equilibrium eq. (10) for the lower part whereby the stress $\sigma_z'(h_o)$ from eq. (16) is taken into account as a boundary condition:

$$\sigma_v' = \sigma_z' (h_o) \, e^{-\lambda \tan\phi (H + D - h_o)/R} + \frac{R\gamma' - c}{\lambda \tan\phi} (1 - e^{-\lambda \tan\phi (h_o - D)/R}) + \gamma_w \, \alpha , \qquad (18)$$

where

$$\alpha = (h_o) \, e^{-\lambda \tan\phi (h_o - D)/R} - h^{**}(D) + \frac{\lambda \tan\phi}{R} \int_D^{h_o} h^{**}(z) \, e^{-\lambda \tan\phi (z - D)/R} \, dz \qquad (19)$$